

Yubao Liu*, Jennifer M. Cram, Chris Davis, Thomas Warner, Simon Low-Nam and Rong Sheu
National Center for Atmospheric Research

1. INTRODUCTION

It is well-known that high-resolution mesoscale models can resolve local details of wind fields and thermal and moisture contrasts forced by underlying inhomogeneities of surface characteristics and topography. Nevertheless, the capabilities of conventional statically initialized mesoscale models are strongly limited by the lack of important mesoscale details and cloud/rain information in their initial conditions due to insufficient observations. The model is forced to experience a “spin-up” process to adjust the dynamic and physical inconsistency between the model and I.C. and to generate the cloud/rain. In this paper, we demonstrate a Real-Time Four-Dimensional Data Assimilation (RTFDDA) method to alleviate this deficiency and improve the short-term forecast for a Utah-centered test region. The system timely collects all available synoptic and asynoptic observations and dynamically nudges them into a nested-grid, 3-domain MM5 model with resolutions of 30/10/3.33km. The details of the system design, model and observation data used can be found in Jennifer et al. (2001). This paper will evaluate impacts of the RTFDDA system on multi-scale data analysis and short-term forecast of local weather by examining different verification statistics and carrying out case studies for two typical weather processes.

2. GENERAL PERFORMANCE

Fig.1 shows evolution of RMS errors of temperature, moisture and winds at surface of the RTFDDA system for all observations on domain 1 during the winter season (Jan., Feb. and Mar.) in 2001. The horizontal axis is hour relative to the forecast, with negative values denoting FDDA periods and positive values for forecasting periods. Evidently, the final FDDA analysis possesses minimum errors for all fields and the errors increase with time.

A large error jump can be seen during preliminary FDDA and 0 - 3 h forecast periods. The reason is that the nudging FDDA method is to artificially drive the model from its wrong states with model constraints (dynamic balance) to a correct state by merging observation information in. The new correct state will be less balanced and the unbalance will be adjusted within certain time. When the

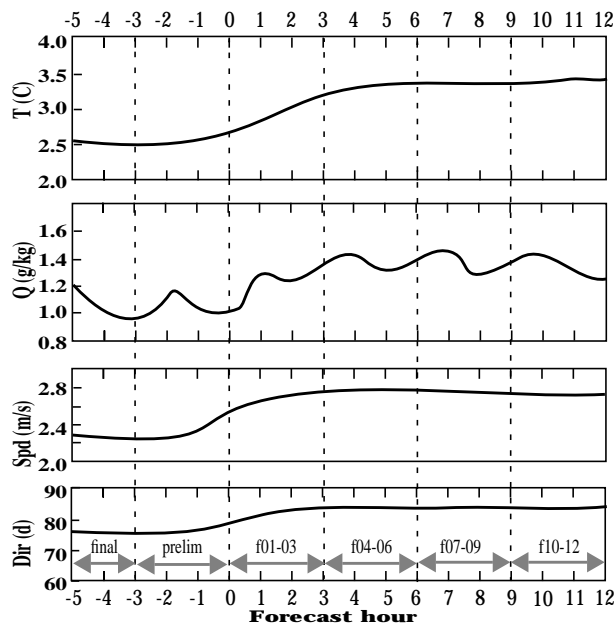


Fig.1 RMSE of surface temperature (T), specific humidity (Q), wind speed (Spd) and wind directions (Dir) on domain 1 at DPG.

model transfers from nudging period to forecast period, the model adjustment will bring significant model error back and meanwhile start accumulate the model system bias.

The model errors change very slowly between 4 - 12 h forecasts. The temperature and moisture forecasts are degraded with time more evidently than the surface wind. Generally, in realtime operation, whenever shorter forecasts are available, it is recommended to use it.

3. SEASONAL, DIURNAL AND SCALE CHANGES

Fig.1 was computed for all observations on domain 1 throughout a three-month winter season of 2001. Such statistics hides many interesting details about the scale variations and seasonal changes of weather situations and underlying properties, as well as the remarkable diurnal evolution of the weather variables. These details are particularly important to understand the model dynamic and physical processes and provide a guide for model improvement in the future. To look into the system performance dependency on the seasonal weather situation and model grid scale, biweekly statistics were conducted twice a month from January 1, 2001. Large systematic changes of the statistic errors can be found between these statistical outputs. For example, Table 1 compares the results

* Corresponding author address: Yubao Liu, National Center for Atmospheric Research, P. O. Box 3000, Boulder, CO 80307-3000. Phone: (303) 497-8211 Email: yliu@ucar.edu

selected from January and April, corresponding to winter and spring, respectively. The statistics were calculated for each forecast period on the two fine mesh domains: D2 and D3. Three features are obvious in the table.

Table 1: RTFDDA surface RMSE averaged for domain 2 and 3 on various forecast periods in January and April, 2001

		T (C)		Q (g/kg)		Spd (m/s)		Dir (d)	
		D2	D3	D2	D3	D2	D3	D2	D3
January	Final	2.74	1.98	0.84	0.37	2.39	2.10	79.4	78.9
	Prelim	2.81	2.06	0.90	0.41	2.53	2.20	80.7	80.2
	F01-03	3.23	2.56	1.18	0.58	2.90	2.58	85.0	86.8
	F04-06	3.44	2.83	1.26	0.64	2.95	2.60	85.8	88.4
	F07-09	3.58	3.00	1.27	0.68	2.95	2.61	86.0	89.3
	F10-12	3.65	3.13	1.26	0.70	2.96	2.62	86.1	88.4
April	Final	1.95	1.55	1.31	0.52	2.28	2.23	73.5	68.5
	Prelim	2.05	1.68	1.33	0.58	2.39	2.30	75.2	70.8
	F01-03	2.41	2.18	1.59	0.85	2.64	2.54	78.6	79.1
	F04-06	2.50	2.31	1.69	0.94	2.68	2.62	79.1	81.9
	F07-09	2.53	2.31	1.73	0.91	2.69	2.68	79.6	82.2
	F10-12	2.56	2.36	1.77	0.95	2.72	2.74	79.8	82.5

Firstly, the fine grid (D3) has much smaller errors than the coarse grid (d2). This indicates that the fine model grid tends to resolve smaller scale weather systems as well as detailed forcing mechanisms from high resolution terrain and land surface characteristics. The conclusion is true generally for all of biweekly statistics obtained so far, for all forecast periods and all weather variables except wind direction. Secondly, the model error increases with forecast time, which is consistent with Fig.1. The third feature is that the system performs better in the spring than in the winter. We believe that an introduction of a simple surface snow and moisture availability scheme (Simon et al., 2001) on March 15 can be one of the most important factors.

To explore the diurnal changes of the model performance, verification scores were calculated relative to the days hour. Again, the statistics are classify into six forecast periods from final FDDA to 10 - 12 h forecasts. The bias and RMS errors of temperature and specific humidity on the domain 3 in the second half of January and first half of April are shown in Fig.2. In the winter month (Fig.2 a-d), the model produces remarkable warm temperature and dry moisture bias. The Largest warm bias occurs during night and morning. Two minimum temperature bias troughs appear at around sunrise and sunset respectively. The evolution of moisture bias is not in same phase of temperature. Large negative moisture bias happens in the daytime and relatively small dry bias

occurs during the night. As aforementioned, the system did not resolve snow cover properly and it used a constant climate land surface moisture availability before March 15. The underestimate of large reflectivity, sublimation and upward moisture flux from the dominant snowcover is mainly responsible to the relatively large warm and dry bias in the winter month.

The large model bias in January actually provides a good opportunity to examine the role of the FDDA. Fig.2 illustrates clearly that the nudging process could successfully assimilate the observation information into the model system and achieve three-dimensional dynamically-consistent high-resolution analysis fields. Starting the model forecast from these FDDA analyses, the model produces more accurate short-term forecast without large "spin-up" problem. During the night time when the large warm bias occurs, the model forecast degrades gradually with increasing forecast time from an error of ~0.7 C for the final FDDA to ~2.3 C for the longest (10 - 12 h) forecasts. The large daytime dry bias has a similar properties. The kicks, one every 3 hours, in the curves of the preliminary FDDA and larger error increase between the preliminary FDDA and 0-3 h forecast result from the balance adjustment discussed in Section 2. The same phenomena appear in the RMS errors of the nudging fields.

In the spring month (Fig.2 e-h), the temperature bias is much less than that in the winter. Due to both less surface snow cover and the introduction of a surface snow and land-surface moisture availability scheme, the large warm and dry bias seen in the winter were reduced remarkably. Like those in the winter, there are two temperature bias troughs taking place around sunrise and sunset times, appearing as the largest cold bias in the spring month. Dry bias starts to develop in the early morning and stays throughout the daytime. In contrast, the model has excessive moisture during the night. The spring month presents also much smaller RMS error for temperature than the winter and the phase of the diurnal evolution appears to be reversed. The evolution of the moisture RMS errors in the spring month are pretty similar to those in the winter. However, the magnitude of the error is a little bit larger.

Finally, it should be pointed out that since the diurnal changes of bias errors of the model variables can go positive and negative, one should look at both bias and RMS errors in order to evaluate the model performance at a specific time or a single model cycle which can starts at varying times. Extra cares should be taken when looking at the bias scores. For instance, in

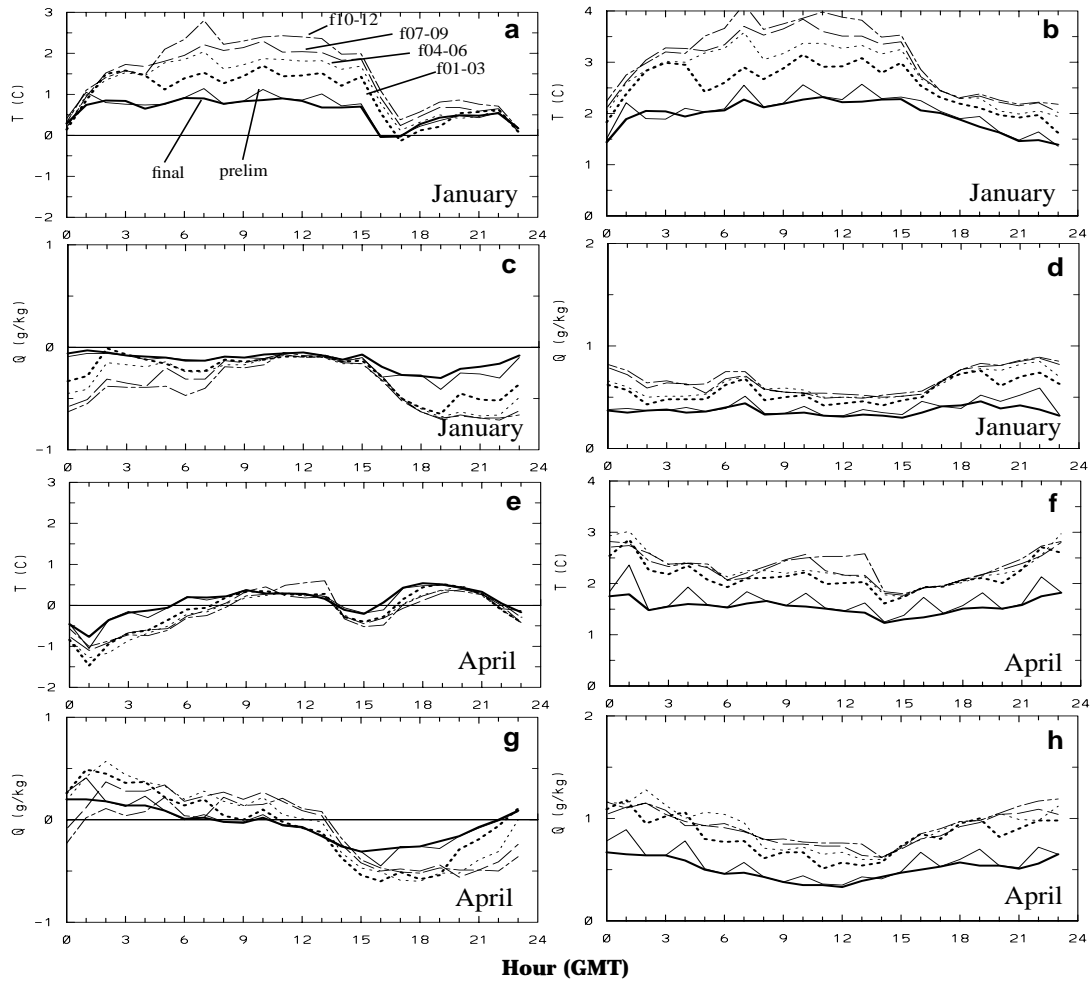


Fig.2 Diurnal change of RTFDDA model surface bias (left column) and RMSE (right) of temperature (T) and specific humidity (Q) on domain 3 in during January 15 - 29 (top 4 panels) and April 01 - 15 (bottom 4 panels), 2001, for each forecast period.

Fig.2g, it looks that the longest forecast performs better than the short forecast and FDDA analysis around 13Z. However, at the same time, their RMS errors (Fig.2h) at the same time shows an opposite conclusion.

4. CASE STUDY

As pointed out at beginning of the paper, there are two common problems in mesoscale numerical simulation and prediction: lack of proper observations to initialize model cloud/rain fields and detailed mesoscale structures. These problems get worse as the model resolution increases. In the present case, the "spin-up" for the mesoscale circulations can be serious due to steep mountains and large contrast of the underlying characteristics in the fine mesh areas. Since the nudging method assimilates the observations into the model equations dynamically, it not only generate good three-dimensional analyses of the nudging variables by driving these model variables directly toward the observed states, but is also capable of obtaining proper

cloud and precipitation information indirectly through the model dynamic and physical processes. The continually running model that resolves the fine scale terrain and land uses can generate the locally-forced mesoscale circulations, with the nudging process further improving these circulation with any available observations. Thus, the continuous RTFDDA cycling provides initial cloud and precipitation fields and detailed mesoscale circulations for short-term forecasts and reduces "spin-up" problem for cloud/rain as well as local circulations. It is our belief that the improvements discussed in previous sections are mostly resulted from this mechanism.

To demonstrate more clearly the advantages of the RTFDDA through improving the model initial conditions for cloud/precipitation and fine scale mesoscale circulations, two cases were selected and parallel comparisons with and without FDDA processes were conducted: one is for March 9 and the other is for April 17, 2001. March 9 was dominated by snowfall from a slow-moving weak mesoscale frontal cycle over Utah

area. In contrast, April 17 is chosen for its clear-sky situation controlled by a upper-air strong ridge and the lower level circulations in domain 2 and 3 were mainly forced by local terrain and land use contrasts.

Table 2: Comparison of model errors on domain 3 between rtfdda forecast and no-fdda forecast on March 9, 2001

		0 - 6 hour			7 - 12 hour	
		E2 FDDA	E1 FCST	E2 FCST	E1 FCST	E2 FCST
T(C)	BIAS	0.04	-0.36	-0.14	1.32	0.63
	RMSE	1.61	2.91	2.23	3.05	2.53
Q(g/kg)	BIAS	0.08	-0.31	0.08	-0.59	0.21
	RMSE	0.47	1.09	0.66	0.94	0.87
SLP(hPa)	BIAS	2.49	3.42	2.77	1.44	1.99
	RMSE	3.22	4.38	3.59	3.61	3.30
SPD(m/s)	BIAS	-0.61	0.20	-0.92	0.92	-0.53
	RMSE	2.29	2.67	2.53	2.71	2.71
DIR	BIAS	-2.19	-3.45	-5.87	-6.93	1.66
	RMSE	55.76	84.65	73.81	94.11	77.35

The verification scores were computed from the parallel model runs for the two cases. In order to remove the artificial effects of the diurnal evolution, the test starts from the middle of the previous day and thus 12 cycles were run for both cases. The FDDA cycles (E2) were divided into 3 periods: 0 - 6 h FDDA, 1 - 6 hour forecast and 7-12 hour forecast. The parallel runs without FDDA (E1) run 13 hours and were divided into two periods: 1-7 hour forecast and 8-13 hour forecast (for convenience, we still called the two periods 0 - 6 hour and 7 - 12 hour forecast respectively). The one hour lag is necessary to make the forecast periods of the runs with and without FDDA coincidently. The bias and RMS errors of temperature, specific humidity, sea level pressure, wind speed and directions for March 9 are shown in Table 2. For all variables in the table, it is obvious that the FDDA analysis (E2 0 - 6 hour FDDA) possesses the least errors, consistent with the general longer term statistics discussed in previous sections. In both 0 - 6 h and 7 - 12 h forecasting periods, the FDDA cycles (E2) perform significantly better than the runs without FDDA (E1).

On March 9 (Table 2), the surface appears to be too dry in E1 throughout the forecast period and a little bit too warmer during the 7 - 12 hour forecast. E2 tends to correct both problems. E2 also achieves a better surface winds prediction, though relatively small. By analyzing various model fields (not shown), it is found that the larger errors in E1 are mainly caused by the phase error of the frontal rain system. In this case, the cloud/rain "spin-up" process leads to slow development of rain in

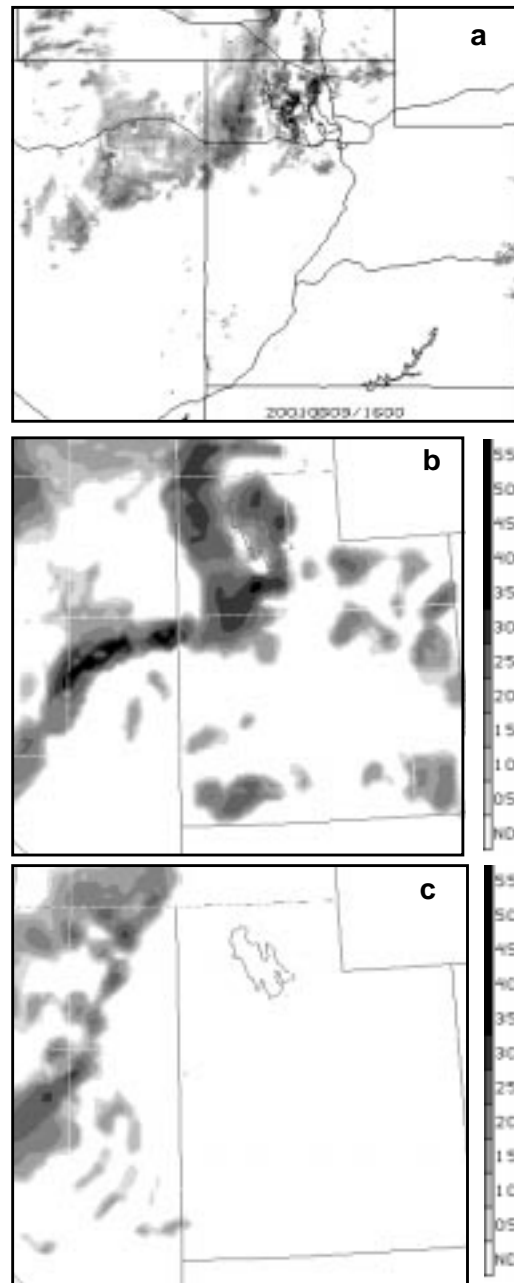


Fig.3 Comparison of radar reflectivity of observation (a), RTFDDA 0-h forecast (b) and "static" 1-h forecast (c) at surface on domain 2, valid at 16Z March 9, 2001.

most cycles. The main frontal rainbands is displaced to the west of the observed band, which results in an overall warm and dry bias for domain 2 and 3. Fig. 3 compares snap-shots of radar reflectivity from E2 0-h forecast, E1 1-h forecast and Utah NOWRAD, valid at 16Z, March 9. Obviously, the FDDA method generated reasonably good precipitation fields to initialize the model forecast. However, in E1, after one hour of "spin-up", it only obtains a weaker rain system, located to the west of the observed reality.

The clear-sky case of April 17 presents mainly locally-developed circulations that are forced by uneven underlying ground heating/cooling and terrain. In domains 2 and 3, various local circulation (with scales

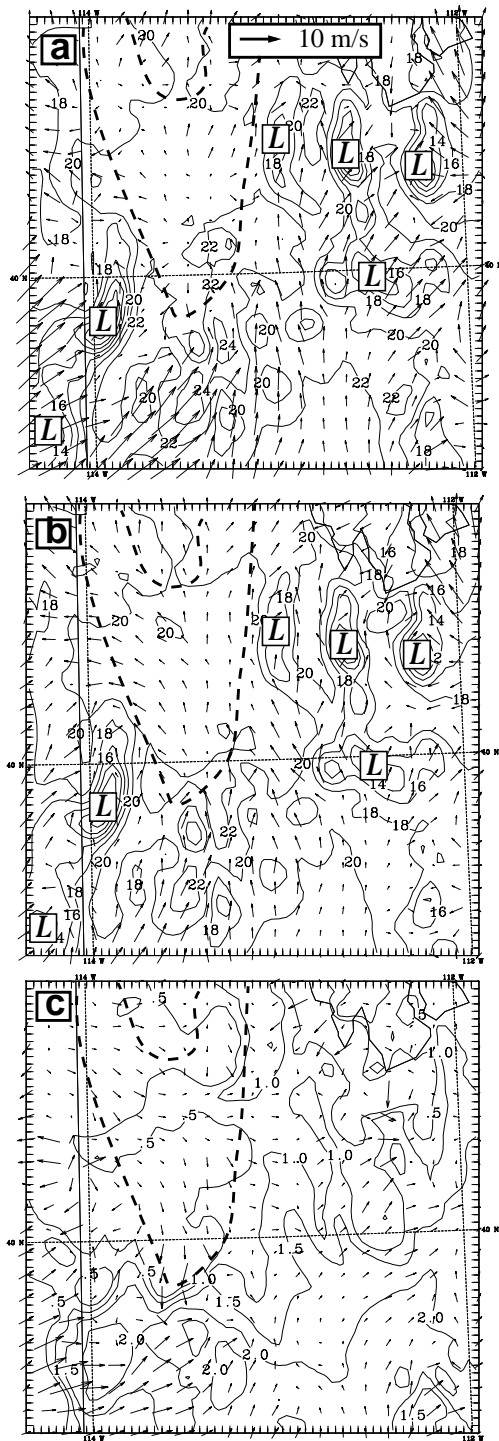


Fig.4 Surface wind vectors and temperature of E2 4-h forecast (a), E1 5-h forecast (b) and (a)-(b) (c) on domain 3, valid at 23Z Apr. 17, 2001. Low temperature center corresponding to major ridges are labelled with "L". The thick dashed line marks roughly the playa-desert boundary.

between 20 and 400 km) systems, including lake-breeze, mountain/valley breeze, salt breeze, and others can be seen clearly during the day (no shown). For this case, surface temperature changes take a controlling role in driving the circulations. The verification results (not shown) indicates that the model system apparently produced significant cold bias in this case, -2.7 and -2.8 C for E1 0 - 6 and 7 - 12 hour forecast, respectively. Comparing E1 and E2, the FDDA analysis (E2 0 - 6 hour FDDA) successfully corrected the bias (to -0.3 C) and forecast a better temperature for both 0 - 6 (a bias of -0.8 C) and 7 - 12 hour (a bias of -1.8 C) forecast.

Since the surface temperature plays a controlling role, E2 forecasts that start with the better initial surface temperature result in a better forecast of the local circulations. This is generally true when we look at the surface circulation plots at various times. Fig.4 compares the surface temperature and wind vectors on domain 3 from the E2 4-h forecast and E1 5-h forecasts, valid at 22Z, April 14, when the thermally driven circulations take maximum intensity. In both E1 and E2, upslope valley breezes can be found around each mountain ridge. In spite of the overall resemblance between the E1 and E2, large discrepancies exist. The most remarkable one can be found in the playa area located in the northwest quadrant of the domain. Playa possesses large heat capacity, high albedo, and high thermal conductivity, which results in much slower and less solar heating than the neighboring desert. Thus, salt breezes develop in the afternoon in clear-sky situation. E2 (Fig.4a) shows a clearer salt-breeze structure than E1 (Fig.4b). Fig.4c indicates that the FDDA cycle (E2) predicts much warmer and better temperature in the desert area to the east and south of the playa, enhancing the flow from playa to the desert. The warmer desert also strengthens the lake breeze from the Salt Lake (northeast corner of the domain) and modifies locally the large scale upslope breeze driven by large ranges in Nevada to the west and valley flow to the southwest of the domain.

REFERENCES

- Cram, J.M., Y. Liu, S. Low-Nam, R-S. Sheu, L. Carson, C.A. Davis, T. Warner, J.F. Bowers, 2001: An operational mesoscale RT-FDDA analysis and forecasting system. *Preprints 18th WAF and 14th NWP Confs.*, Ft. Lauderdale, AMS, Boston, MA.
- Low-Nam, S., C.A. Davis, J.M. Cram, Y. Liu, and R.-S. Sheu, 2001: Use of a snow prediction scheme in a mesoscale real-time FDDA system. *Preprints 18th WAF and 14th NWP Confs.*, Ft. Lauderdale, AMS, Boston, MA.